


Volume 15, 2018

ISSN 1544-0479

Journal of Natural Fibers

Published in this journal online
Number 4

 Taylor & Francis
Taylor & Francis Group

[Submit an article](#)

[New content alerts](#)

[RSS](#)

[Citation search](#)

[Current issue](#) [Browse list of issues](#)

< **Volume 15, 2018** Vol 14, 2017 Vol 13, 2016 Vol 12, 2015 Vol 11, 2014 >

[See all volumes and issue](#)

< Issue 4 Issue 3 Issue 2 **Issue 1** >

Original Articles

Article

Optimization of Eco-Friendly Reactive Dyeing of Cellulose Fabrics Using Supercritical Carbon Dioxide Fluid with Different Humidity >

Juan Zhang, Huanda Zheng & Lajiu Zheng

Pages: 1-10

Published online: 07 Apr 2017

[Abstract](#) | [Full Text](#) | [References](#) | [PDF \(962 KB\)](#)

75 Views

0 CrossRef citations

0 Altmetric

[Submit an article](#)

[New content alerts](#)

[RSS](#)

[Citation search](#)

[Current issue](#) [Browse list of issues](#)

Article

Studies on Mechanical and Morphological Characterization of Developed Jute/Hemp/Flax Reinforced Hybrid Composites for Structural Applications >

Vijay Chaudhary, Pramendra Kumar Bajpai & Sachin Maheshwari

Pages: 80-97

Published online: 22 May 2017

[Abstract](#) | [Full Text](#) | [References](#) | [PDF \(2344 KB\)](#)

128 Views

5 CrossRef citations

0 Altmetric

Article

The Influence of Chemical Treatments on Cantala Fiber Properties and Interfacial Bonding of Cantala Fiber/Recycled High Density Polyethylene (rHDPE) >

Wijang Wisnu Raharjo, Rudy Soenoko, Yudy Surya Irawan & Agus Suprpto

Pages: 98-111

Published online: 14 Jun 2017

[Abstract](#) | [Full Text](#) | [References](#) | [PDF \(1578 KB\)](#)

48 Views

0 CrossRef citations

0 Altmetric

Article

Effect of Thermal Aging and Chemical Treatment on Tensile Properties of Coir Fiber >

R Manjula, NV Raju, RPS Chakradhar & Jobish Johns

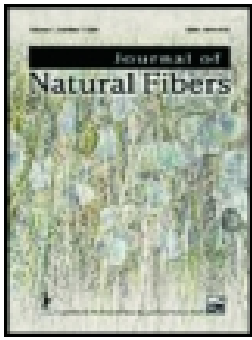
Pages: 112-121

Published online: 16 Oct 2017

89 Views

0 CrossRef citations

0



The Influence of Chemical Treatments on Cantala Fiber Properties and Interfacial Bonding of Cantala Fiber/Recycled High Density Polyethylene (rHDPE)

Wijang Wisnu Raharjo, Rudy Soenoko, Yudy Surya Irawan & Agus Suprpto

To cite this article: Wijang Wisnu Raharjo, Rudy Soenoko, Yudy Surya Irawan & Agus Suprpto (2017): The Influence of Chemical Treatments on Cantala Fiber Properties and Interfacial Bonding of Cantala Fiber/Recycled High Density Polyethylene (rHDPE), Journal of Natural Fibers, DOI: [10.1080/15440478.2017.1321512](https://doi.org/10.1080/15440478.2017.1321512)

To link to this article: <http://dx.doi.org/10.1080/15440478.2017.1321512>



Published online: 14 Jun 2017.



Submit your article to this journal [↗](#)



View related articles [↗](#)



View Crossmark data [↗](#)



The Influence of Chemical Treatments on Cantala Fiber Properties and Interfacial Bonding of Cantala Fiber/Recycled High Density Polyethylene (rHDPE)

Wijang Wisnu Raharjo^{a,b}, Rudy Soenoko^b, Yudy Surya Irawan^b, and Agus Suprpto^c

^aMechanical Engineering Department, Sebelas Maret University, Surakarta, Indonesia; ^bMechanical Engineering Department, Brawijaya University, Malang, Indonesia; ^cMechanical Engineering Department, Merdeka University, Malang, Indonesia

ABSTRACT

The influence of chemical treatments on the properties of cantala fiber as well as on the quality of the interfacial bonding of cantala fiber/rHDPE was investigated. The fibers were treated with alkali, silane, and a combination of both. The results showed that the loss of hemicellulose and lignin after the alkali treatment, and the presence of a silane layer on the fiber surface after the silane or alkali-silane treatment, improved the thermal stability, surface energy, and IFSS. The highest surface energy of 45.37 mN/m was obtained during the alkali treatment (NF12). The alkali-silane treatment with 0.75% wt of silane (NSF075) gave the highest thermal stability and IFSS value.

KEYWORDS

Cantala fiber; chemical treatment; interfacial bonding; surface energy; thermal stability

关键词

肯太拉麻纤维; 化学处理; 界面结合; 表面能; 热稳定性

摘要

本文研究了化学处理对肯太拉麻纤维性能的影响以及肯太拉麻纤维/rHDPE 界面结合质量的影响。纤维分别用碱、硅烷和两者的组合进行处理。结果表明, 碱处理后损失了半纤维素和木质素, 硅烷或碱-硅烷处理后纤维表面硅烷层的存在提高了热稳定性、表面能和 IFSS。在碱处理 (NF12) 中获得的最高表面能为 45.37 mN/m。用 0.75% (重量比) 硅烷 (NSF075) 进行碱-硅烷处理可得到最高的热稳定性和 IFSS 值。

Introduction

Awareness of the importance of preserving the environment has encouraged the development of alternative materials that are environmentally friendly and recyclable, such as natural fiber/thermoplastic composites. The natural fibers act as a reinforcement, while the thermoplastic serves as the binder material. Natural fibers have several advantages such as low price, low density, abundance, biodegradability, and high toughness (Mohanty, Misra, and Drzal 2001; Valadez-Gonzalez et al. 1999). In view of all these factors, natural fibers have the potential to replace synthetic fibers in polymeric composites.

Agave cantala Roxb, as shown in Figure 1(a), is a natural fiber-producing crop. In Indonesia, this plant is cultivated in East Java, Central Java, Yogyakarta, West Java and North Sumatra. Cantala fiber (Figure 1b) is mostly used as rope, for weaving, and crafts. As 55% of the fiber is comprised of cellulose, it can be developed as reinforcement in polymer composites (Palungan et al. 2015). However, like other natural fibers, the cantala fiber has some drawbacks, namely its relatively poor adhesion with polymers (Dittenber and GangaRao 2012), relatively low thermal stability (Bledzki and Gassan 1999), and high moisture absorption (Cao, Sakamoto, and Goda 2007).

CONTACT Wijang Wisnu Raharjo  m_asyain@yahoo.com  Mechanical Engineering Department, Faculty of Engineering, Sebelas Maret University (UNS), Jl. Ir. Sutami 36A, Surakarta 57126, Indonesia.

Color versions of one or more of the figures in the article can be found online at www.tandfonline.com/WJNF.

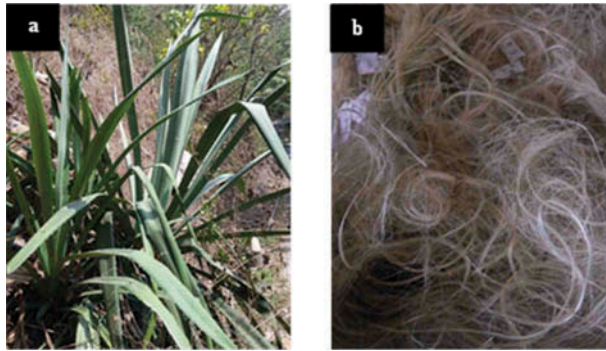


Figure 1. (a) Agave cantala roxb and (b) cantala fibers, Raharjo et al.

Interfacial bonding plays an important role in determining the mechanical properties of a composite (Zhao and Takeda 2000). The existence of a hydroxyl group (OH) in natural fibers prevents good bonding with the hydrophobic polymer and obstructs the effectiveness of the load transfer between the fibers and the matrix (Gan, Tian, and Yi 2014). Various chemical treatments have been carried out to improve the interfacial bonding (Li, Tabil, and Panigrahi 2007; Sawpan, Pickering, and Fernyhough 2011b). Among the various treatment methods, alkali and silane are the most widely used treatments. Alkali treatment creates mechanical interlocking and increases the area of exposed cellulose on the fiber surface, whereas silane treatment generates a coating on the fiber surface that adheres to the matrix. The effectiveness of silane in improving the interfacial bonding depends on its concentration. A low concentration will lead to inadequate coupling between the fiber and the matrix, while an excessive concentration will cause the silane to agglomerate on the fiber surface (Gyoung et al. 2010). Treatment with a suitable alkali-silane concentration will enable the creation of good bonding between the fiber and the matrix. However, only a few works have considered the concentration of silane for improving interfacial bonding. In addition, there is not much information in relation to the utilization of cantala fiber as reinforcement for polymer composites. In this study, alkali, silane, and a combination of both were applied to the cantala fiber. The effectiveness of the fiber treatment and the silane concentration was investigated through the properties of the fiber such as its chemical composition, density, surface morphology, thermal behavior, wettability, and the IFSS of the fiber/rHDPE.

Materials and methods

Materials

The cantala fiber was supplied by CV Rami Kencana, Kulonprogo, Indonesia. The fibers were extracted from the leaves of the Agave cantala Roxb using the mechanical retting method. Prior to the treatment, the fibers were heated at 110°C for 45 minutes. The rHDPE flakes were obtained from CV Vanilla Plastik, Sukoharjo, Indonesia. The material has a melting temperature ranging from 108.5 to 139.5°C with a heating rate of 10°C/min, a density of 1,014 kg/m³, and a melt flow index (MFI) of 2.43 g/10 min at 180°C (Raharjo, Sukanto, and Anwar 2015).

Sodium hydroxide (NaOH) from Merck was used for the fiber surface treatment. Amino ethylamino propyl tri-methoxy silane (AAMS) was used as a coupling agent between the fiber and the matrix. It was supplied by Dow Corning. It has a specific gravity of 1.03 with a viscosity of 5 mm²/s. The chemical structure of the silane coupling agent is shown in Figure 2.

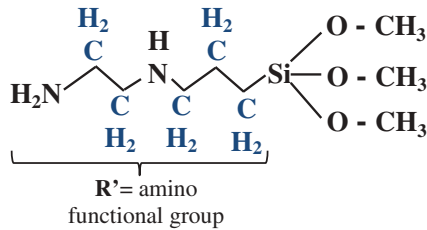


Figure 2. Chemical structures of AMMS, Raharjo et al.

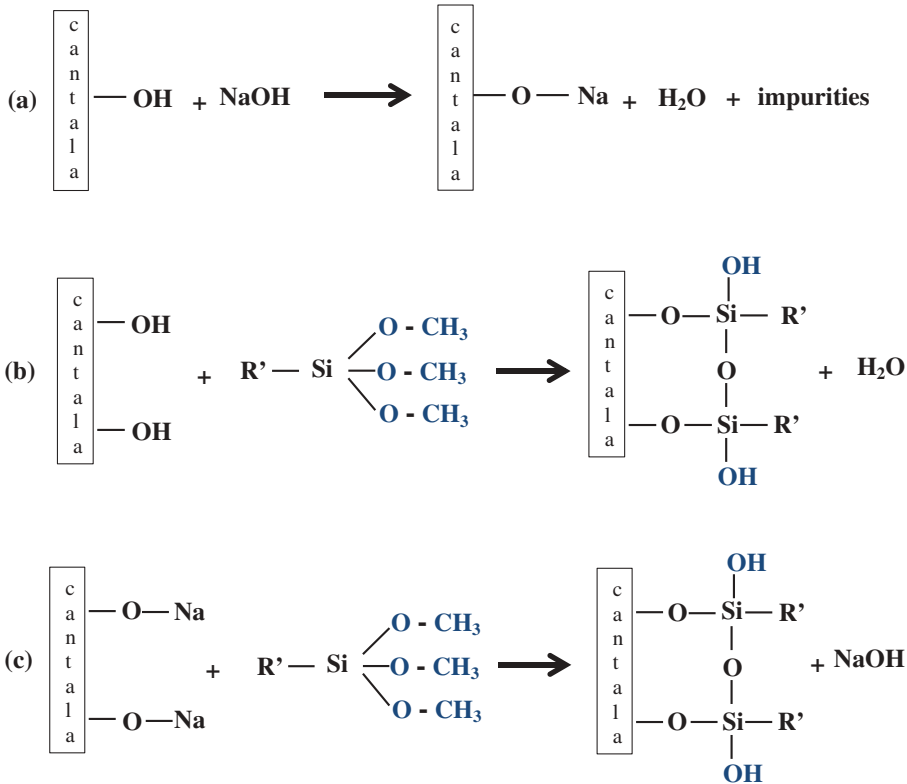


Figure 3. (a) Reaction in alkali treatment, (b) reaction in silane treatment, (c) reaction in alkali-silane treatment, Raharjo et al.

Alkali treatment

The alkali treatment was conducted by immersing the cantala fiber in 2 wt% of NaOH solution at room temperature for 12 hours. The chemical reaction of the alkali-treated fibers is displayed in Figure 3(a). Furthermore, the fibers were rinsed several times until pH~7 was reached. The wet fibers were dried at room temperature for 48 hours, followed by heating in an oven at 70°C for 10 hours.

Silane treatment

The silane treatment was performed by soaking the cantala fiber in a silane solution at a concentration ranging from 0.25 to 1 wt% in distilled water at intervals of 0.25%. Acetic acid was added to the silane solution to obtain a pH within the range of 3–4. The cantala fiber was soaked in the solution for four hours. After that, the wet fibers were kept at room temperature for 48 hours before being

Table 1. A nomenclature used for various treated and untreated cantala fibers.

Treatment type	Code	Description
Untreated	UF	Fiber without treatment
Alkali	NF12	Fiber treated with 2 wt% NaOH aqueous solution for 12 hours
Silane (SF)	SF025	Fiber treated with 0.25 wt% silane aqueous solutions
	SF050	Fiber treated with 0.50 wt% silane aqueous solutions
	SF075	Fiber treated with 0.75 wt% silane aqueous solutions
	SF1	Fiber treated with 1.00 wt% silane aqueous solutions
Alkali-Silane (NSF)	NSF025	Silane treatment of alkali treated fibers in 0.25 wt% silane aqueous solutions
	NSF050	Silane treatment of alkali treated fibers in 0.50 wt% silane aqueous solutions
	NSF075	Silane treatment of alkali treated fibers in 0.75 wt% silane aqueous solutions
	NSF1	Silane treatment of alkali treated fibers in 1.00 wt% silane aqueous solutions

ssdried at 70°C for 10 hours. The schematic diagram of the reaction involved in the production of the silane-treated fibers is presented in [Figure 3\(b\)](#).

Alkali and silane treatment

In the alkali-silane treatment, after the cantala fiber had been treated initially with NaOH solution, it was immersed in a silane solution. Here, the silane concentration ranged in between 0.25 to 1 with intervals of 0.25%. The chemical reaction of the cantala fiber following the alkali-silane treatment is displayed in [Figure 3\(c\)](#). The nomenclatures for the various surface treatments of the cantala fiber used in this work are presented in [Table 1](#).

Chemical analysis

The chemical composition of the fibers was evaluated by chemical analysis. In this analysis, the percentage values of α -cellulose and hemicellulose were determined using ASTM D1103-60, while the lignin content was evaluated according to SNI0492-2008.

Density measurement

The fiber density measurement was in accordance with ASTM D3800. The average of ten measurements was used to determine the fiber density. Diesel fuel, with a density of 0.85 g/cm³, was used as a solution.

Fourier Transform Infrared Spectrometry (FTIR)

The alteration in the functional groups in the treated and untreated fibers was observed by Shimadzu IR Prestige-21. The fibers were ground into powder and then mixed with potassium bromide (KBr). The ratio of fiber powder to KBr was 1:200. The transmittance spectra were recorded in wavelenghts of between 500 and 4000 cm⁻¹ at a resolution of 2 cm⁻¹ for 45 scans.

Thermogravimetric Analysis (TGA)

The thermal stability of the untreated and treated cantala fiber was analyzed using thermogravimetric (TG) techniques. The measurements were performed using a Perkin Elmer Diamond TG/DTA. The scanning of each specimen with a weight of around 5 mg was done at a temperature of 30–1000°C with a heating rate of 10°C/min.

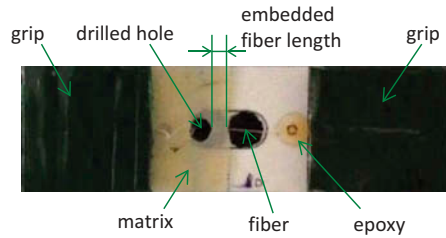


Figure 4. Pullout test sample, Raharjo et al.

Single-fiber pull-out test

The IFSS of the cantala fiber-rHDPE was investigated by a single-fiber pull-out test. The sample was prepared by putting the cantala fiber between two sheets of rHDPE film on an aluminium mold. Furthermore, the sample was heated at a temperature of 150°C for 15 min at a pressure of 1.5 bars using a hot press. The length of the embedded fiber in the matrix was controlled by drilling a hole. Finally, the sample was mounted on a paperboard before being tested (Figure 4). The pull-out test was conducted on a universal testing machine JTM-UTS510. The gauge length was set at 10 mm with a crosshead speed of 0.10 mm/min at ambient conditions.

Scanning electron microscopy

The surface morphology of the untreated and treated fibers was examined by environmental scanning electron microscopy (ESEM) type VEGA 3 TESCAN.

Contact angle measurement

The measurement of the contact angle was conducted by photographing liquid droplets on the fiber surface using an Olympus ZX7 microscope. The droplet volume was controlled at 1.5 ml using a micropipette. Distilled water and ethylene glycol were used to investigate the fiber surface properties. The fiber surface energy was estimated from the value of the contact angle (θ) using the Owens–Wendt method, as indicated by Eq. (1) (Owens 1969):

$$\gamma_{L(1+\cos\theta)} = 2 \frac{\gamma_S^d \gamma_L^d}{\gamma_S^d + \gamma_L^d} + 2 \frac{\gamma_S^p \gamma_L^p}{\gamma_S^p + \gamma_L^p} \quad (1)$$

where the superscripts, d and p, are related to the dispersive and polar surface energy, respectively, and the subscripts S and L for the solid and liquid circumstances are correlated as well.

Result and discussion

Surface morphology

The SEM images of the untreated (UF) and alkali-treated fibers (NF12) are presented in Figure 5. The UF surface (Figure 5a) was covered by impurities such as waxes and fats, so the surface topography of the UF was smoother than that of the NF12. On the contrary, the NF12 surface looked clean with many grooves (Figure 5b). This indicated that the alkali treatment had effectively eliminated the impurities and hemicellulose from the fiber surface. A similar result was also obtained by other studies (Zhou, Cheng, and Jiang 2014).

Figure 6 shows the surface structure of the silane-treated fiber (SF). During the treatment, the silane molecules built a link with the fiber constituents. So, at the end of the process, a layer of silane was present on the fiber surface. The added concentration of silane encouraged an increase in the

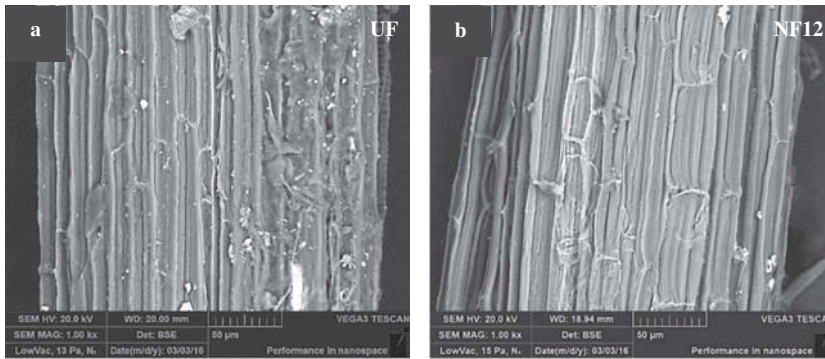


Figure 5. (a) Indicates UF, 5 (b) indicates NF12, Raharjo et al.

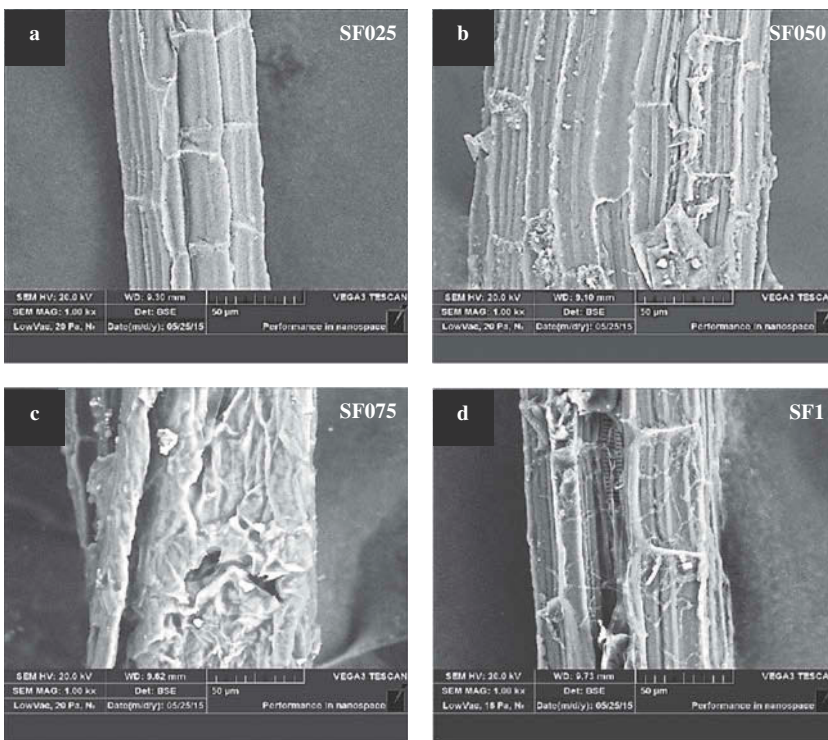


Figure 6. (a) Indicates SF025, 6(b) indicates SF050, 6(c) indicates SF075, 6(d) indicates SF1, Raharjo et al.

deposition of silane on the fiber surface. The surface morphology of the alkali-silane-treated fiber (NSF) is displayed in [Figure 7](#). After the treatment, the NSF surface became rougher compared to that of the UF and NF12. In addition, the surface topography of the fibers after undergoing the alkali-silane treatment was similar to that of the silane-treated fibers. This observation was in line with the result of previous studies (Gan, Tian, and Yi 2014).

Fiber density

[Table 2](#) presents the density of the untreated and treated cantala fiber. It was observed that all the treatments resulted in an increase in the fiber density. In the case of alkali treatment, the impurities and

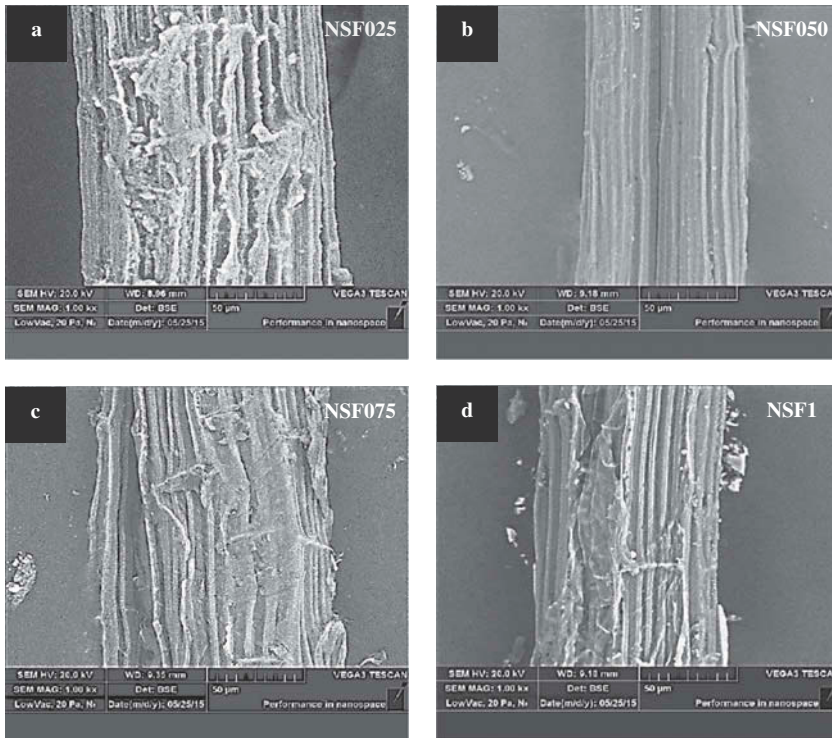


Figure 7. (a) Indicates NSF025, 7 (b) indicates NSF050, 7 (c) indicates NSF075, 7 (d) indicates NSF1, Rahrjo et al.

Table 2. The average density of the untreated and treated cantala fibers.

No	Treatment type	Code	Density (g/cm^3)
1	Untreated	UF	1.056 ± 0.0145
2	Alkali	NF12	1.377 ± 0.0189
3	Silane (SF)	SF025	1.098 ± 0.0201
4		SF050	1.120 ± 0.0428
5		SF075	1.125 ± 0.0230
6	Alkali-Silane (NSF)	SF1	1.130 ± 0.0125
7		NSF025	1.372 ± 0.0136
8		NSF050	1.374 ± 0.0124
9		NSF075	1.380 ± 0.0223
10		NSF1	1.382 ± 0.0177

low-density amorphous components were removed from the fibers. Besides, the new structure of cellulose component, i.e., cellulose-II, which is more stable and compact compared to that of cellulose-I will be formed. This mechanism was also notified by (Jacob et al. 2005). The elimination of amorphous material and the formation of a denser structure will reduce the volume of fiber and increase the weight of fiber, so that, the density of the NF12 was higher than that of the UF. An increase in fiber density was also found to have occurred in hemp fibers (Sawpan, Pickering, and Fernyhough 2011a) and Borassus fruit fiber (Boopathi, Sampath, and Mylsamy 2012) following treatment with alkali.

In silane and alkali-silane treatments, the silane layer on the fiber surface encouraged an increase in fiber density. The NSF had a higher density than the UF, SF, and NF12. The alkali treatment cleaned off all the impurities from the fiber surface, and this elimination of fiber surface defects was followed by a coating of silane, which prompted the enhancement of the NSF density. The increase in the silane concentration caused an increase in the density of the SF and

Table 3. A number of fiber constituents (weight %) presents in the treated fibers.

Treatment type	Code	Alfa-cellulose	Hemicellulose	Lignin
Untreated	UF	59.47	27.71	9.11
Alkali	NF12	68.74	15.76	7.96
Silane (SF)	SF025	58.24	28.14	8.84
	SF050	59.60	24.97	11.42
	SF075	60.95	27.08	10.25
	SF1	63.63	32.27	7.35
	Alkali-Silane (NSF)	NSF025	66.7	23.96
	NSF050	65.8	25.41	12.1
	NSF075	66.5	23.57	12.36
	NSF1	69.83	19.57	10.92

NSF. This was due to the addition of a silane deposit on the fiber surface. In another work, treatment with silane and alkali-silane also increased the density of hemp fibers (Sawpan, Pickering, and Fernyhough 2011a).

Chemical analysis

Table 3 presents the chemical composition of the untreated and treated fibers. After the alkali treatment, the percentage of hemicellulose and lignin in the NF12 was lower than in the UF. The cleaning away of hemicellulose and lignin from the fiber surface enhanced the cellulose content in the NF12. A similar tendency was observed when napier grass fibers were treated with 2 and 5 wt% of NaOH aqueous solutions (Reddy et al. 2012).

For the silane treatment, the chemical composition of the SF was similar to that of the UF. There was no significant change in the amount of cellulose and hemicellulose as the silane solution was unable to dissolve the cellulose, hemicellulose and lignin. Similar results were also found for husks (Tran, Bénézet, and Bergeret 2014). In contrast, after the alkali-silane treatment, the hemicellulose content was reduced in the fibers but the cellulose content increased compared to the UF. This was because the impurities and hemicellulose were eroded during the alkali treatment. This encouraged the enhancement of the total percentage of cellulose after the second treatment using silane. The increasing silane concentration during both the silane and alkali-silane treatments had no significant effect on the alteration of the chemical composition in the SF and NSF, respectively. This was due to the fact that silane can not remove hemicellulose and lignin from the fiber surface (Kabir et al. 2013). During silane treatment, the enrichment of silane concentration encouraged the slight increase in hemicellulose content. This enhancement was contributed by a coupling between silane molecules and hemicellulose which were deposited on the fiber surfaces. The similar phenomenon occurred on the alkali-silane treatment, silane would form a coupling with cellulose which was presented on the fiber surface after alkali treatment. Therefore, the relative amount of cellulose would be slight increasing.

FTIR Analysis

The spectra of the untreated and treated cantala fibers are displayed in Figure 8. The functional groups appeared in the fiber component, and their related IR spectra (wave numbers) are listed in Table 4. The peak around 3400 cm^{-1} indicated the vibration of the hydroxyl group (OH) in the cellulose of the cantala fibers (Orue et al. 2015; Sawpan, Pickering, and Fernyhough 2011a). Both the SF and NSF led to the overlapping vibration of the hydroxyl group (OH) derived from cellulose and silane. It was marked by the enhancement of the intensity in the region.

The peak around 2850 cm^{-1} was caused by the symmetrical stretching of CH_2 (Le Troedec et al. 2008). This peak appeared in all the fibers. Meanwhile, the peak at 1732 cm^{-1} was assigned to the

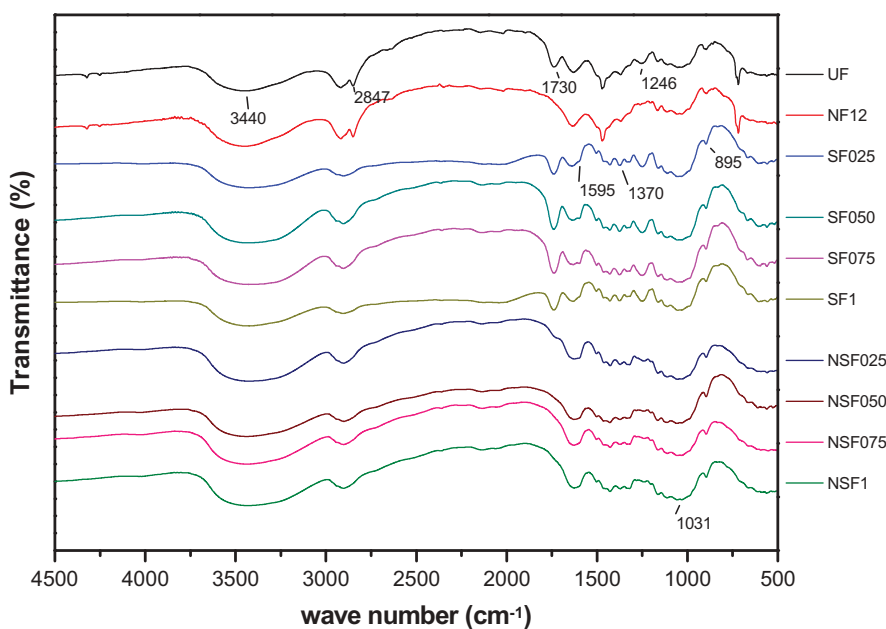


Figure 8. FT-IR Spectra of fiber, Raharjo et al.

Table 4. Infrared transmittance peaks of fiber constituents.

Wave number	Functional groups	References
3400	-OH stretching vibration from the cellulose, and silane	(Orue et al. 2015; Sawpan, Pickering, and Fernyhough 2011b)
2850	CH ₂ symmetrical stretching (Waxes and oils)	(Le Troedec et al. 2008)
1732	>C = O Stretching of a carboxylic acid or ester (hemiselulose)	(Le Troedec et al. 2008; Sawpan, Pickering, and Fernyhough 2011b)
1370	-Si-O-Cellulose	(Valadez-Gonzalez et al. 1999)
1246	C-O Stretching of acetyl (lignin)	(Sawpan, Pickering, and Fernyhough 2011b)
1031	-Si-O-Si- asymmetric stretching	(Valadez-Gonzalez et al. 1999; Zhou, Cheng, and Jiang 2014)
895	-Si-OH (silanol groups)	(Valadez-Gonzalez et al. 1999; Tran, Bén��zet, and Bergeret 2014)

carbonyl (C = O) groups present in hemicellulose (Le Troedec et al. 2008; Sawpan, Pickering, and Fernyhough 2011a). After the alkali and alkali-silane treatments, the removal of hemicellulose from the fiber surface caused this peak to disappear. However, as the silane treatment was unable to remove the hemicellulose, the SF had a similar peak to the UF. The peak at 1246 cm⁻¹ was related to the C-O stretching of acetyl (lignin) (Sawpan, Pickering, and Fernyhough 2011a). In NF12 and NSF, lignin was discarded from the cantala fiber surface, so the peak did not appear. Meanwhile, there were no changes in the FTIR spectra of the SF as the silane treatment was unable to eliminate lignin from the fiber.

In Figure 8, the new peaks that appeared at 1595 cm⁻¹ are believed to have emerged from the vibration of the NH₂ groups in the organosilane agent. It indicated that the silane had been chemically grafted onto the fiber surface. Similar results were obtained with sisal fibers using aminoethyl amino propyltrimethoxysilane (Orue et al. 2015; Zhou, Cheng, and Jiang 2014). The absorption bands at 1370 cm⁻¹ confirmed the presence of Si-O from the Si-O-cellulose bond in the SF and NSF (Valadez-Gonzalez et al. 1999). The presence of a new peak at 1031 cm⁻¹ could be identified as the Si-O groups from Si-O-Si bonds (Valadez-Gonzalez et al. 1999; Zhou, Cheng, and Jiang 2014). These suggested that

the intermolecular condensation between the adjacent Si-OH groups had been completed. It showed the reaction between the hydrolysed silane and the cantala fiber. The observed peaks at 895 cm^{-1} for the SF and NSF were associated with the formation of silanol groups during the hydrolysis of silane (Tran, Bén  zet, and Bergeret 2014; Valadez-Gonzalez et al. 1999). As for the SF and NSF, the new peaks at 1595 and 1031 cm^{-1} did not change significantly when the silane concentration increased. This may have been because the molecular interaction between the silane and the fiber component was weak, so the changes on the fiber surface were too small to be detected by FTIR.

Thermal analysis of fibers

The thermogravimetric analysis (TGA) and differential thermal analysis (DTA) curves of the untreated and treated fibers are presented in Figure 9 and summarized in Table 5. It can be seen that the fiber degradation was indicated by three stages. In the first stage, between $30\text{--}220^\circ\text{C}$, an initial weight loss was observed in the untreated and treated fibers (Figure 9a). In the UF, the weight loss of about 5.6%, which appeared at around 120°C , was related to surface water evaporation. After the alkali treatment, the weight loss of the NF12 is found to be lower than that of the UF (Table 5). This indicated that the alkali treatment had transformed the fibers to make them less hydrophilic. On the contrary, the weight loss in the SF and NSF was higher than that in the UF. It was attributed to the removal of absorbed moisture by the cantala fiber and the generation of moisture by self-condensation reactions.

The second stage had two sub-stages. In the first sub-stage, between 220 and 300°C , the initial decomposition temperature (IDT) of the UF was found to be around 220°C (Figure 9a), with a weight loss of 5.8% (Table 5). After the alkali treatment, the IDT of the NF12 shifted to a higher temperature, i.e., 265°C (Figure 9b). This enhancement was associated with the removal of the amorphous material, which was more sensitive to heat than the crystalline component. In the case of the SF12 and NSF12, there was an increase in the IDT in comparison to the UF. It indicated that a silane layer on the surface of the UF and NF12 protected the fibers from thermal decomposition at the higher temperature. A similar result was observed by (Singha and Rana 2012) for grewia optiva fibers treated with 3-aminopropyltriethoxysilane.

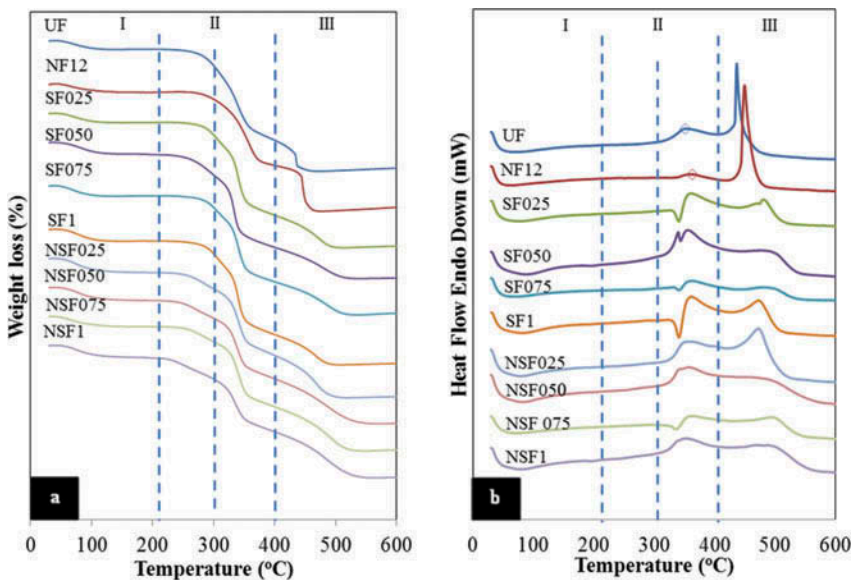


Figure 9. (a) Thermogravimetric analysis (TGA), 9(b) differential thermal analysis (DTA), Raharjo et al.

Table 5. Thermogravimetric result of treated and untreated cantala fibers.

Treatment type	Code	Temperature range (°C)			
		30–200	200–300	300–400	400–600
		Temp (°C)/ % wt loss	IDT (°C)/% wt loss	PDT (°C)/% wt loss	PDT (°C)/% wt loss
Untreated	UF	120/5.6	220/5.8	346.5/51.1	449.5/88.5
Alkali	NF12	153/5.3	265/5.4	359.3/42.1	465.5/86.8
Silane (SF)	SF025	135/6.3	256/6.7	357.8/62.4	488.9/91
	SF050	141/7.8	238/9.2	357.3/65.5	506.3/92.1
	SF075	129/7	252/7.4	356.5/58.5	501.2/86
	SF1	134/7.9	242/8.2	359.1/65	481.1/91.2
Alkali-Silane (NSF)	NSF025	138/9.1	243/10.2	347.9/52.5	483.3/92.4
	NSF050	135/8.3	232/9.5	352.5/54.05	501/86.2
	NSF075	134/6.6	243/7.6	354.4/53.7	507.1/88.7
	NSF1	125/7.3	220/9	345.8/48.2	507/85.2

The second sub-stage started from 300 to 400°C. It was associated with the decomposition of cellulose (Figure 9b). After the alkali treatment, the UF peak at 346.5°C shifted to a higher temperature (359.3°C). This was related to the removal of a vast majority of the amorphous material. A similar result was observed by (Orue et al. 2015; Zhou, Cheng, and Jiang 2014) for sisal fibers. In the case of SF and NSF, the peak decomposition temperature (PDT) of cellulose shifted to the higher temperature. This indicated that a silane layer on the surface of the SF and NSF enhanced the heat resistance and the decomposition temperature of the fibers.

The third stage, between 400 and 600°C, was associated with the combustion of the degraded material in the previous stage and the decomposition of lignin (Joseph et al. 2003). For the UF, the DTA curve showed a maximum weight loss rate at 449.5°C. After the alkali treatment, the PDT shifted to a higher temperature (465.5°C), thereby suggesting that the thermal stability of the NF12 had improved significantly. In the case of the SF and NSF, the PDT appeared at the higher temperatures (481–507°C). The silane layer prevented structural damage to the fibers, thereby enhancing the thermal stability of the SF and NSF. When the silane concentration was enhanced, the highest thermal stability was obtained for the SF050 with silane treatment and the NSF075 with alkali-silane treatment. This was because the SF05 and NSF075 had better silane-fiber bonding than the others. The excess silane concentration could have encouraged the agglomeration of silane on the fiber surface, thereby weakening the interface between the fibers and silane.

Contact angle and surface energy

The potential of the fiber-matrix adhesion can be predicted from the wettability of the fibers. To evaluate the wetting behavior of fibers, the contact angle and surface energy values are discussed. Table 6 shows the contact angle and surface energy for the untreated and treated cantala fiber. In water and ethylene glycol, the untreated fibers had a higher contact angle with lower surface energy compared to the treated fibers. This indicated that the UF was hydrophobic with a low polarity, so it was difficult for it to be wetted. The existence of a non-polar material, such as wax, oil, pectin, and lignin, on the fiber surface caused the UF to become hydrophobic.

During the alkali treatment, the non-polar components were cleaned from the fiber surface, as observed in the chemical analysis, FTIR, and TGA. The elimination of the non-polar components in the NF12 caused an increase in the polarity from 35.44 to 43.47 mN/m and in the surface energy from 37.57 to 45.37 mN/m. A similar case was found in hemp fibers (Pietak et al. 2007). The silane modification and alkali-silane treatment also augmented the polar components and the surface energy. The enhancement was caused by the reaction between the polar components of the silane and hydroxyl groups in the cantala fiber. This phenomenon was in agreement with the results

Table 6. Surface energies of untreated and treated fibers as derived from contact angle measurements.

Material	Contact angle in distilled water (deg)	Contact angle in ethylene glycol (deg)	Dispersion (mN/m)	Polarity (mN/m)	Surface energy (mN/m)
UF	72.96	71.47	2.13	35.44	37.57
NF12	66.57	66.18	1.90	43.47	45.37
SF025	72.31	70.98	2.08	36.31	38.39
SF050	71.84	71.38	1.72	38.13	39.85
SF075	71.96	69.85	2.47	35.46	37.93
SF1	71.70	68.51	3.05	34.09	37.14
NSF025	71.94	70.00	2.39	35.73	38.11
NSF050	69.88	67.34	2.78	36.81	39.59
NSF075	69.52	68.94	1.86	40.23	42.09
NSF1	69.61	66.74	2.96	36.58	39.54

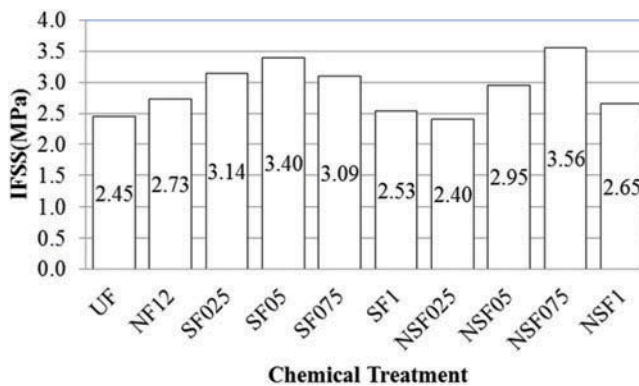
reported by (Feresenbet, Raghavan, and Holmes 2003). The highest surface energy of 45.37 mN/m was obtained after the alkali treatment.

With the added silane concentration, the maximum increase in surface energy was found in SF05 for the silane treatment and in NSF075 when the alkali-silane treatment was used. This was caused by an increase in the polar units of amino silane grafted onto the fibers. The excessive silane concentration could have encouraged the enhancement of surface roughness, thereby leading to a decrease in the surface energy. These observations were in line with the results of the morphological, chemical and FTIR analyses.

Interfacial Shear Strength (IFSS)

The interfacial shear strength (IFSS) of the cantala fiber/rHDPE as a function of the fiber treatment is depicted in Figure 10. It was found that all the fiber treatments enhanced the IFSS. For the UF/rHDPE, the IFSS value was about 2.4 MPa and it increased to 2.7 MPa after the alkali treatment. This was due to the removal of the non-cellulose material from the fibers to increase the interfacial fiber-matrix bonding. A similar tendency was observed by (Gan, Tian, and Yi 2014; Orue et al. 2015).

Similar to the alkali treatment, silane also significantly enhanced the IFSS value of the cantala fiber/rHDPE. The IFSS of the SF/rHDPE was higher than that of the UF/rHDPE. The IFSS of the rHDPE composite based on the SF025, SF050, SF075, and SF1-treated fibers were 3.1 MPa, 3.4 MPa, 3.1 MPa, and 2.5 MPa, respectively. As for the silane treatment, the IFSS of the SF05/rHDPE (3.4 MPa) increased by 41.7% compared to that of the UF/rHDPE (2.4 MPa). The chemical bonding between the rHDPE matrix and the amino groups of silane, which were embedded in the fiber

**Figure 10.** Average IFSS, Raharjo et al.

surface, led to an increase in the IFSS value. A similar observation was also reported by (Orue et al. 2015) for sisal/PLA, and by (Gan, Tian, and Yi 2014) for sisal/PP.

In the alkali-silane treatment, the IFSS of the NSF/rHDPE was in the range of 2.4–3.6 MPa, which was higher than that of the UF/rHDPE. The alkali treatment produced roughness in the fiber surface and increased the exposed area of the OH groups on the cellulose, thereby improving the quality of the interaction between silane and the fibers. Besides that, it generated a covalent bond between the silane group and the matrix chain. The highest IFSS values were found for SF050 (3.4 MPa) and NSF075 (3.6 MPa) for the silane treatment and alkali-silane treatment, respectively. The excess silane concentration would have encouraged the formation of a weak boundary layer. Therefore, the IFSS value decreased at the higher silane concentration.

Conclusion

Alkali, silane, and a combination of both treatments were used to improve the properties of cantala fiber as well as the interfacial adhesion of cantala fiber/rHDPE. All the treatments resulted in an increase in the fiber density, thermal stability, surface energy, and IFSS. The amorphous materials, such as hemicellulose and lignin, were mostly removed by the alkali treatment, as confirmed by the chemical analysis, FTIR, and TGA. The alkali treatment produced the highest surface energy of 45.37 mN/m. After the silane and alkali-silane treatment, the FTIR and TGA confirmed the presence of the amino group. It indicated that the silane had been successfully grafted onto the fiber surface. The presence of a silane layer improved the thermal stability, surface energy, and the IFSS of the cantala fiber/rHDPE. The highest thermal stability was found in the NSF075, i.e., up to 507.1°C. The improvement in the interaction between the fiber and the matrix increased the IFSS of the treated cantala fiber/rHDPE. The highest IFSS value of 3.6 MPa was found in the NSF075.

References

- Bledzki, A. K., and J. Gassan. 1999. Composites reinforced with cellulose based fibres. *Progress in Polymer Science* 24:221–74. doi:10.1016/S0079-6700(98)00018-5.
- Boopathi, L., P. S. Sampath, and K. Mylsamy. 2012. Investigation of physical, chemical and mechanical properties of raw and alkali treated borassus fruit fiber. *Composites Part B* 43 (8):3044–52. doi:10.1016/j.compositesb.2012.05.002.
- Cao, Y., S. Sakamoto, and K. Goda. 2007. Effects of heat and alkali treatments on mechanical properties of kenaf fibers. 16Th International Conference on Composite Materials, Kyoto, Japan, 8–13 July, 1–4.
- Dittenber, D. B., and H. V. S. GangaRao. 2012. Critical review of recent publications on use of natural composites in infrastructure. *Composites Part A* 43 (8):1419–29. doi:10.1016/j.compositesa.2011.11.019.
- Feresenbet, E., D. Raghavan, and G. A. Holmes. 2003. The influence of silane coupling agent composition on the surface characterization of fiber and on fiber-matrix interfacial shear strength. *The Journal of Adhesion* 79 (7):643–65. doi:10.1080/00218460309580.
- Gan, H. L., L. Tian, and C. H. Yi. 2014. Effect of sisal fiber surface treatments on sisal fiber reinforced polypropylene (PP) composites. *Advanced Materials Research* 906:167–77. doi:10.4028/www.scientific.net/AMR.906.
- Gyoung, J., S. Young, S. Jin, G. Hyun, and J. Hyeun. 2010. Effects of chemical treatments of hybrid fillers on the physical and thermal properties of wood plastic composites. *Composites Part, A* 41 (10):1491–97. doi:10.1016/j.compositesa.2010.06.011.
- Jacob, M., S. Joseph, L. A. Pothan, and S. Thomas. 2005. A study of advances in characterization of interfaces and fiber surfaces in lignocellulosic fiber-reinforced composites. *Composite Interfaces* 12 (1–2):95–124. doi:10.1163/1568554053542115.
- Joseph, P. V., K. Joseph, S. Thomas, C. K. S. Pillai, V. S. Prasad, G. Groeninckx, and M. Sarkissova. 2003. The thermal and crystallisation studies of short sisal fibre reinforced polypropylene composites. *Composites Part A* 34:253–66. doi:10.1016/S1359-835X(02)00185-9.
- Kabir, M. M., H. Wang, K. T. Lau, and F. Cardona. 2013. Effects of chemical treatments on hemp fibre structure. *Applied Surface Science* 276:13–23. doi:10.1016/j.apsusc.2013.02.086.
- Le Troedec, M., D. Sedan, C. Peyratout, J. P. Bonnet, A. Smith, R. Guinebretiere, V. Gloguen, and P. Krausz. 2008. Influence of various chemical treatments on the composition and structure of hemp fibres. *Composites Part A* 39 (3):514–22. doi:10.1016/j.compositesa.2007.12.001.

- Li, X., L. G. Tabil, and S. Panigrahi. 2007. Chemical treatments of natural fiber for use in natural fiber-reinforced composites: A review. *Journal of Polymers and the Environment* 15 (1):25–33. doi:10.1007/s10924-006-0042-3.
- Mohanty, A. K., M. Misra, and L. T. Drzal. 2001. Surface modifications of natural fibers and performance of the resulting biocomposites: An overview. *Composite Interfaces* 8 (5):313–43. doi:10.1163/156855401753255422.
- Orue, A., A. Jauregi, C. Peña-Rodríguez, J. Labidi, A. Eceiza, and A. Arbelaz. 2015. The effect of surface modifications on sisal fiber properties and sisal/poly (Lactic Acid) interface adhesion. *Composites Part B* 73:132–38. doi:10.1016/j.compositesb.2014.12.022.
- Owens, D. K. 1969. Estimation of the surface free energy of polymers. *Journal of Applied Polymer Science* 13:1741–47. doi:10.1002/app.1969.070130815.
- Palungan, M. B., R. Soenoko, Y. S. Irawan, and A. Purnowidodo. 2015. Mechanical properties of king pineapple fiber (Agave Cantula Roxb) as A result of fumigation treatment. *Australian Journal of Basic and Applied Sciences* 9:560–63.
- Pietak, A., S. Korte, E. Tan, A. Downard, and M. P. Staiger. 2007. Atomic force microscopy characterization of the surface wettability of natural fibres. *Applied Surface Science* 253 (7):3627–35. doi:10.1016/j.apsusc.2006.07.082.
- Raharjo, W. W., H. Sukanto, and M. Anwar. 2015. Effect of soaking time in alkali solution on the interfacial shear strength of cantala fiber/recycled HDPE composites. *Materials Science Forum* 827:375–80. doi:10.4028/www.scientific.net/MSF.827.375.
- Reddy, K. O., C. U. Maheswari, M. Shukla, and A. V. Rajulu. 2012. Chemical composition and structural characterization of napier grass fibers. *Materials Letters* 67 (1):35–38. doi:10.1016/j.matlet.2011.09.027.
- Sawpan, M. A., K. L. Pickering, and A. Fernyhough. 2011a. Effect of various chemical treatments on the fibre structure and tensile properties of industrial hemp fibres. *Composites Part A* 42 (8):888–95. doi:10.1016/j.compositesa.2011.03.008.
- Sawpan, M. A., K. L. Pickering, and A. Fernyhough. 2011b. Effect of fibre treatments on interfacial shear strength of hemp fibre reinforced polylactide and unsaturated polyester composites. *Composites Part A* 42 (9):1189–96. doi:10.1016/j.compositesa.2011.05.003.
- Singha, A. S., and A. K. Rana. 2012. Effect of aminopropyltriethoxysilane (APS) treatment on properties of mercerized lignocellulosic grewia optiva fiber. *Journal of Polymers and the Environment* 21 (1):141–50. doi:10.1007/s10924-012-0449-y.
- Tran, T. P. T., J. Bénézet, and A. Bergeret. 2014. Rice and einkorn wheat husks reinforced Poly(lactic Acid) (PLA) biocomposites: Effects of alkaline and silane surface treatments of husks. *Industrial Crops and Products* 58:111–24. doi:10.1016/j.indcrop.2014.04.012.
- Valadez-Gonzalez, A., J. M. Cervantes-UC, R. Olayo, and P. J. Herrera-Franco. 1999. Chemical modification of henequen fibers with an organosilane coupling agent. *Composites Part B* 30:321–31. doi:10.1016/S1359-8368(98)00055-9.
- Zhao, F. M. M., and N. Takeda. 2000. Effect of interfacial adhesion and statistical fiber strength on tensile strength of unidirectional glass fiber /epoxy composites. Part I : Experiment results. *Composites Part A* 31:1215–24. doi:10.1016/S1359-835X(00)00086-5.
- Zhou, F., G. Cheng, and B. Jiang. 2014. Effect of silane treatment on microstructure of sisal fibers. *Applied Surface Science* 292:806–12. doi:10.1016/j.apsusc.2013.12.054.